Nephrol Dial Transplant (2006) 1 of 9
doi:10.1093/ndt/gfl071

NDT
Nephrology Dialysis Transplantation

Orginal Article

Gene profiling of polycystic kidneys

Gisela Schieren[2], Brigitta Rumberger[1], Marinella Klein[1], Clemens Kreutz[3], Jochen Wilpert[1], Marcel Geyer[1], Daniel Faller[3], Jens Timmer[3], Ivo Quack[2], Lars Christian Rump[2], Gerd Walz[1] and Johannes Donauer[1]

[1]Renal Division, Department of Internal Medicine, University Hospital, Freiburg, [2]Renal Division, Department of Internal Medicine, Ruhr-University Hospital Bochum at Marienhospital Herne and [3]Freiburg Center for Data Analysis and Modeling, Department of Physics, University of Freiburg, Freiburg, Germany

Abstract

Background. While the genetic basis of autosomal dominant polycystic kidney disease (ADPKD) has been clearly established, the pathogenesis of renal failure in ADPKD remains elusive. Cyst formation originates from proliferating renal tubular epithelial cells that de-differentiate. Fluid secretion with cyst expansion and reactive changes in the extracellular matrix composition combined with increased apoptosis and proliferation rates have been implicated in cystogenesis.

Methods. To identify genes that characterize pathogenical changes in ADPKD, we compared the expression profiles of 12 ADPKD kidneys, 13 kidneys with chronic transplant nephropathy and 16 normal kidneys using a 7 k cDNA microarray. RT–PCR and immunohistochemical techniques were used to confirm the microarray data.

Results. Hierarchical clustering revealed that the gene expression profiles of normal, ADPKD and rejected kidneys were clearly distinct. A total of 87 genes were specifically regulated in ADPKD; 26 of these 87 genes were typical for smooth muscle, suggesting epithelial-to-myofibroblast transition (EMT) as a pathogenetic factor in ADPKD. Immunohistology revealed that smooth muscle actin , a typical marker for myofibroblast transition, and caldesmon were mainly expressed in the interstitium of ADPKD kidneys. In contrast, up-regulated keratin 19 and fibulin-1 were confined to cystic epithelia.

Conclusion. Our results show that the end stage of ADPKD is associated with increased markers of EMT, suggesting that EMT contributes to the progressive loss of renal function in ADPKD.

Correspondence and offprint requests to: Johannes Donauer, Medizinische Klinik IV, Hugstetter Strasse 55, 79106 Freiburg, Germany. Email: donauer@med1.ukl.uni-freiburg.de

Keywords: ADPKD; end-stage renal disease; epithelial-to-myofibroblast transition; gene expression; microarray

Introduction

Autosomal dominant polycystic kidney disease (ADPKD) is a common hereditary disease, caused by mutations of either *PKD1* or *PKD2*. The onset of the disease is poorly defined, but the findings of microcysts in embryonal kidneys suggest that cyst formation starts during renal development (see [1] for a recent review) and progresses continuously in adulthood. Most individuals with *PKD1* mutations experience renal failure in their fifth decade of life, while the onset of end-stage renal disease (ESRD) is delayed by about two decades in patients with *PKD2* mutations.

Polycystin-1, the protein encoded by *PKD1*, is a large integral membrane protein with a domain architecture suggesting a function in cell–cell or cell–matrix interaction [2].

Polycystin-2 is a member of the calcium-permeable subfamily of TRP channels, and forms a complex with polycystin-1 [3,4]. Both polycystin-1 and polycystin-2 are present in the primary cilium of tubular epithelial cells, and the raise in intracellular calcium mediated by cilial bending requires the presence of both proteins [5].

Despite these recent advances in understanding the function of polycystin-1 and polycystin-2, the pathogenesis of cyst formation and particularly, the development of ESRD in ADPKD have remained elusive. Less-than-terminal differentiation of epithelial cells that line the cysts, persistent proliferation due to mislocalization of EGF receptors, stimulation of proto-oncogenes, and cyst expansion as a result of inappropriate fluid secretion have been implicated

to explain, why a few hundred cysts cause complete destruction of the renal parenchyma [6]. However, increased apoptosis rates detected in the normal tissue surrounding renal cysts suggest that additional factors account for the progressive loss of renal function [7].

We chose cDNA microarrays to screen for mechanisms possibly involved in cyst formation and/or progression of the disease. Expression profiling revealed smooth muscle actin (SMA), caldesmon, sarcospan-2, fibulin-1, 22 kDa smooth muscle protein and other genes involved in epithelial-to-myofibroblast transition (EMT) to be specifically up-regulated in ADPKD. RT–PCR and immunohistochemistry confirmed our results on RNA and protein level and suggest that the absence of functional polycystins results in increased expression of EMT genes.

Subjects and methods

Microarrays

cDNA microarrays were produced and processed essentially according to the Stanford protocol described by Eisen and Brown [8]. Approximately 7000 annotated genes from the RZPD (Resource Center and Primary Database, Berlin, Germany) were obtained as bacterial stocks. Plasmids were purified using the Qiagen 96-well Turbo Kit (Qiagen, Hilden, Germany), and inserts were purified by PCR using vector primers flanking the individual inserts (5′-CTG CAA GGC GAT TAA GTT GGG TAA C -3′ and 5′-GTG AGC GGA TAA CAA TTT CAC ACA GGA AAC AGC-3′). PCR products were purified by ethanol precipitation and resuspended in H_2O. Aliquots were transferred into 384-well plates, dried and resuspended in 3 × SSC or DMSO 10% to a final concentration of ∼40 ng/µl. Printing was performed on aminosilane-coated slides (CMT-GAP II Slides, Corning, NY, USA), using an arrayer that was assembled according to specifications by the Stanford group using software kindly provided by J. de Risi (http://cmgm.stanford.edu/pbrown).

Tissue Samples

Informed consent was obtained from all patients, according to the study protocol approved by the ethics committee of Freiburg University. Elective transplant removal was performed on all renal graft recipients at the Freiburg transplant centre after transplant failure and reinitiation of renal replacement therapy. Normal renal tissue was obtained from tumour nephrectomies; tumour infiltration was excluded by histology. Nephrectomies of cystic kidneys were done in most cases pre-transplant or in context with complications caused by the organ such as bleeding or pain. Tissue samples (approximately 1 × 1 × 2 cm in size or 3 × 3 cm in cystic kidneys) were removed and either snap-frozen in liquid nitrogen for RNA isolation or fixed in 4% paraformaldehyde for immunohistochemistry immediately after organ removal. After the exclusion of insufficient or tumour-contaminated samples, 12 kidneys with end-stage PKD, 13 chronically rejected renal allografts, and 16 normal renal tissues were analysed by microarrays.

RNA preparation

Frozen tissue was homogenized in 4 M guanidinium isothiocyanate with 0.72% ß-mercaptoethanol using a polytron (PT-MR2100, Kinematica AG, Lucerne, Switzerland). Total RNA was subsequently purified on a cesiumchloride gradient. After ethanol precipitation, RNA was resuspended at a concentration of 0.4–4 µg/µl and stored at −80°C.

Hybridization

All hybridizations were performed in the presence of an equal amount of reference RNA (Stratagene, La Jolla, CA, USA) as published by Boldrick *et al*. [9]. Two micrograms of either tissue or reference-RNA were transcribed into cDNA in the presence of Cy3- and Cy5-labelled dUTP, using Superscript II reverse transcriptase (Invitrogen, Carlsbad, CA, USA). All other steps, including hybridization, were performed following the protocol published by Brown *et al*. (see http://cmgm.stanford.edu/pbrown for details); a PCR-purification kit (Qiagen, Hilden, Germany) was used for cDNA purification after dye-labelling.

Data analysis

Signal intensities were measured by an Axon 4000A scanner using GenePix 3.0 software (Axon Instruments Inc, Union City, CA, USA). The experimental design included a colour-reversal experiment for every tissue sample to correct for dye-specific effects. Initially, the log-ratio of measured Cy3/Cy5 values obtained from the image analysis software was computed. Global normalization of expression values was performed by adjusting the data to zero median and unit variance in order to obtain an identical distribution of the overall gene expression. Taking the mean of the expression values of the dye-swap experiments allows correction for dye-specific effects. Following an approach proposed by Dudoit *et al*. [10], the computed expression ratios should not depend on the intensity of the spots. Hence, a smooth non-linear least-squares fit was computed to correct for an intensity-dependent bias. A two sample *t*-test was used for a statistical analysis of differentially expressed genes. In order to adjust the obtained *P*-values, the method by Benjamini and Hochberg [11] was applied to control for multiple testing. Hierarchical clustering was performed using the R-statistical software package (www.r-project.org).

Semiquantitative RT–PCR

Total RNA (1µg) from all normal and polycystic kidneys was purified with the RNase free DNase set (Qiagen, Hilden, Germany), and reversely transcribed into cDNAs using oligo (dT) 12–18 primer and Superscript II reverse transcriptase (Invitrogen, Carlsbad, CA, USA). Each PCR was carried out with GAPDH as an internal control in each reaction vial. The following primers were used (5–3′): GAPDH—GTCT TCTGGGTGGCAGTTAG and TGGAAATCCCATCACC ATCT; Keratin 19—GTGCCACCATTGAGAACTCC and AGCTCTTCCTTCAGGCCTTC; Fibulin-1—AGTAACC CGTCTTGCATTCG and GGGCATACATGCATCAAC AC; Calponin—TCACCCCATACTTGGTGATG and GG AGCTGAGAGAGTGGATCG; Caldesmon—TTGTTGGG TCGAACTCCTTC and GAATCCTTGGGACAGGTGAC.

The amplification cycle consisted of a hot start at 94°C for 5 min, followed by multiple cycles of denaturation at 94°C at 1 min, annealing at 58°C for 1 min and elongation at 72°C for 2 min. Cycle number was adjusted to mRNA expression level of the different genes. The PCR products were run on a 3% agarose gel and evaluated in relation to the corresponding GAPDH band using Scion Image Software (Scion, Frederick, ML, USA).

Immunochemistry

Genes of different fold expression changes were randomly selected for validation by immunochemistry. Tissue samples were fixed in 4% paraformaldehyde, dehydrated and paraffin-embedded. After rehydration procedure 10 µm tissue sections were incubated with 5% horse serum in phosphate-buffered saline (PBS), pH7.4, for 1 h at room temperature and then incubated with the respective primary antibody, diluted in PBS–BSA 1%, for 16 h at 4°C. Sections were rinsed three times with PBS–BSA 1%, followed by incubation with the respective rhodamine-red conjugated secondary antibody for 30 min at room temperature. After extensive washing with PBS–BSA 1% stained sections were examined with a Zeiss microscope.

The following antibodies were used: affinity-purified murine monoclonal antibody against pancytokeratin, affinity-purified murine monoclonal antibody against CD3 (used as negative control for murine monoclonal antibodies) (Sigma-Aldrich,Taufkirchen, Germany); horse serum and affinity-purified murine monoclonal antibodies against SMA, affinity-purified murine monoclonal antibody against keratin 19 (DakoCytomation Hamburg, Germany); affinity-purified polyclonal antibody from goat against fibulin-1 (Santa Cruz, Heidelberg, Germany) and affinity-purified murine monoclonal antibody against caldesmon (Biomol, Hamburg, Germany), Rhodamine Red-X AP-conjugated donkey anti-goat IgG, Rhodamine Red-X AP-conjugated goat anti-mouse (Dianova, Hamburg, Germany).

Results

Hierarchical clustering differentiates polycystic kidneys, normal kidney and chronically rejected transplant kidneys

To characterize end-stage ADPKD, we used samples of PKD kidneys that were removed during organ transplantation, and yielded a minimal amount of 50 µg of total RNA. Twelve samples fulfilled this criterion, and were included in our analysis. To identify genes that are specifically regulated in ADPKD, we used non-affected renal tissue removed during 16 tumour nephrectomies, and 13 samples from patients with end-stage renal allograft failure. To compare individual kidneys, each microarray analysis was performed against a standard reference RNA. In addition, each hybridization was repeated with inversed dyes to correct for the effects of different dye-incorporation, and to reduce the statistical error. Stringent data analysis of 16 control kidneys, 12 polycystic kidneys and 13 renal transplants with chronic transplant failure, entailing more than 550 000 single measurements, permitted the identification of a distinct gene expression pattern for polycystic kidneys in comparison with normal kidneys and end-stage renal transplants. Approximately 16% genes were differentially regulated in ADPKD compared with normal kidney tissue ($P < 0.0005$), and approximately 14.5% of those were altered more than 3-fold. To select genes specifically regulated in ADPKD, we limited our analysis to genes that were at least 1.5-fold up- or down-regulated compared with normal kidney tissue ($P < 0.05$). Furthermore, we eliminated genes generally altered in ESRD by applying the same criteria ($P < 0.05$ and minimal 1.5-fold regulation) between ADPKD and chronically rejected kidneys. A total of 87 genes met these criteria (Table 1).

Table 1. Eighty-seven regulated genes differentiate polycystic kidneys in renal failure from normal kidneys and chronically rejected transplants ($P < 0.05$). Only genes that are at least 1.5-fold up- or down-regulated are shown

PKD/control	ID	Name	Function
7,13	AF026692	Frizzled related protein	Signalling
6,10	M81349	Amyloid A protein	Lipid metabolism
5,35	M18767	Complement subcomponent C1s	Immunresponse
5,26	D86090	Prostaglandin E receptor	Immunresponse
4,33	M95787	Smooth muscle protein (SM22)	Cytoskeleton
4,01	AF063002	LIM protein SLIMMER	Homeostasis
4,01	U53445	DOC1	Unknown
3,97	AF034208	RIG-like 7-1	Unknown
3,90	AF053944	Aortic carboxypeptidase-like protein	Cytoskeleton
3,89	X92963	Ubiquitin conjugating enzyme	Protein metabolism
3,82	Y11710	Extracellular matrix collagen XIV	Adhesion/ECM
3,74	Y00503	Keratin 19	Adhesion/ECM
3,70	AB003184	ISLR	Adhesion/ECM
3,70	M63603	Phospholamban	Cytoskeleton
3,69	M63835	IgG Fc receptor I	Immunresponse
3,68	AF279145	Endothelial marker 8 precursor (TEM8)	Protein metabolism
3,53	U27768	Regulator of G-protein signalling 4	Signalling
3,46	M55593	Type IV collagenase	Adhesion/ECM

Continued

Table 1. Continued.

PKD/control	ID	Name	Function
3,37	X03350	Alcohol dehydrogenase-beta	Carbohydrate metabolism
3,34	M14219	Chondroitin/dermatan sulfate protein	Adhesion/ECM
3,31	U10550	Gem GTPase (gem)	Signalling
3,13	D78014	Dihydropyrimidinase related protein 3	DNA metabolism
3,09	Z36748	Serotonin receptor	Signalling
3,04	U69263	Matrilin-2 precursor	Adhesion/ECM
3,04	X53742	Fibulin-1 B	Adhesion/ECM
3,03	S74445	Cellular retinoic acid-binding protein	Signalling
3,02	M33216	Smooth muscle alpha-actin	Cytoskeleton
2,95	U25278	ERK5	Signalling
2,86	AB018311	Latrophilin 3	Signalling
2,82	M34057	Transforming growth factor-beta 1	Signalling
2,82	AL110197	Tissue inhibitor of metalloproteinase 2	Adhesion/ECM
2,81	AB000220	Semaphorin E	Signalling
2,79	M19480	Follistatin	Differentiation
2,79	Y18207	Protein phosphatase 1 (PPP1R5)	Protein metabolism
2,77	AF016028	Sarcospan-2 (SPN2)	Cytoskeleton
2,65	AF334829	Mitochondrial endoribonuclease	Protein metabolism
2,65	AF151909	Palladin	Cytoskeleton
2,54	AJ239383	Immunoglobulin heavy chain	Immunresponse
2,49	AJ223812	Caldesmon	Cytoskeleton
2,48	M12792	Steroid 21-hydroxylase	Steroid metabolism
2,47	X61950	Endothelin-1 receptor	Signalling
2,46	X51405	Carboxypeptidase E	Protein metabolism
2,46	U33849	Lymphoma proprotein convertase	Protein metabolism
2,43	U67058	Proteinase activated receptor	Signalling
2,39	D79997	Maternal embryonic leucine zipper kinase	Protein metabolism
2,39	AF035752	Caveolin-2	Signalling
2,38	M22430	RASF-A PLA2	Lipid metabolism
2,34	AB007972	Protein phosphatase 1, regulatory (inhibitor) subunit 12B	Cytoskeleton
2,34	D17408	Calponin	Cytoskeleton
2,32	U60060	FEZ1	Transcription
2,31	U44103	GTP binding protein Rab9	Homeostasis
2,26	AF000421	TTF-I interacting peptide	Franscription
2,26	U25138	Maxi K potassium channel beta subunit	Homeostasis
2,20	M83216	Caldesmon	Cytoskeleton
2,17	X04412	Gelsolin	Cytoskeleton
2,15	AJ001014	RAMP1	Homeostasis
2,14	X07874	CD2 gene	Immunresponse
2,14	U47671	T-box transcription factor TBX5	Transcription
2,11	Y00638	Leukocyte common antigen	Immunresponse
2,09	J00124	Epidermal keratin	Cytoskeleton
2,08	AF041434	Prenylated protein tyrosine phosphatase hPRL-3	Signalling
2,06	AF093119	Fibulin-4	Adhesion/ECM
2,05	U66198	Fibroblast growth factor homologue	Signalling
1,97	D84143	Ig-light chain	Immunresponse
1,90	AB014598	Hephaestin	Ion transport
1,82	M91196	DNA-binding protein	Transcription
1,80	U67784	Orphan G protein-coupled receptor	Signalling
1,80	Y07512	Type I beta-cGMP-dependent kinase	Signalling
1,78	U39817	Human Bloom's syndrome protein (BLM)	DNA metabolism
1,74	U39447	Copper monamine oxidase	Oxygen and radical metabolism
1,74	AB002364	ADAMTS-2 precursor	Adhesion/ECM
1,74	M21812	Myosin light chain	Cytoskeleton
1,73	U79299	Olfactomedin-related ER located protein	Unknown
1,68	M64716	Ribosomal protein S25	Protein metabolism
1,67	AF039291	Lysyl oxidase	Adhesion/ECM
1,65	U77594	Tazarotene-induced gene 2	Signalling
1,64	S65738	Actin depolymerizing factor	Cytoskeleton
1,64	AF032108	Integrin alpha-7	Adhesion/ECM
1,59	AI565209	MHC class 1 region	Immunresponse
1,59	AF017418	Homeobox protein MEIS2	Transcription
1,56	AF001862	FYN-binding protein	Signalling
1,56	D16494	Very low-density lipoprotein	Lipid metabolism
1,51	J02907	Serine protease gene	Protein metabolism
0,65	AF035269	Phosphatidylserine-specific phospholipase A1	Lipid metabolism
0,62	AB002342	WNK lysine deficient protein kinase 1	Homeostasis
0,36	AF098484	Napsin 1 precursor	Protein metabolism
0,22	M79463	PML-2	Transcription

Two-dimensional cluster analysis of these 87 genes separated ADPKD kidneys from normal and transplanted kidneys (Figure 1). One branch of the dendrogram contained all ADPKD kidneys, while the other branch contained three subgroups: 12 of 14 normal kidneys, seven transplants (T×1, T×5, T×7, T×10, T×11, T×13, T×14), and two normal kidneys clustered with the remaining five transplant kidneys

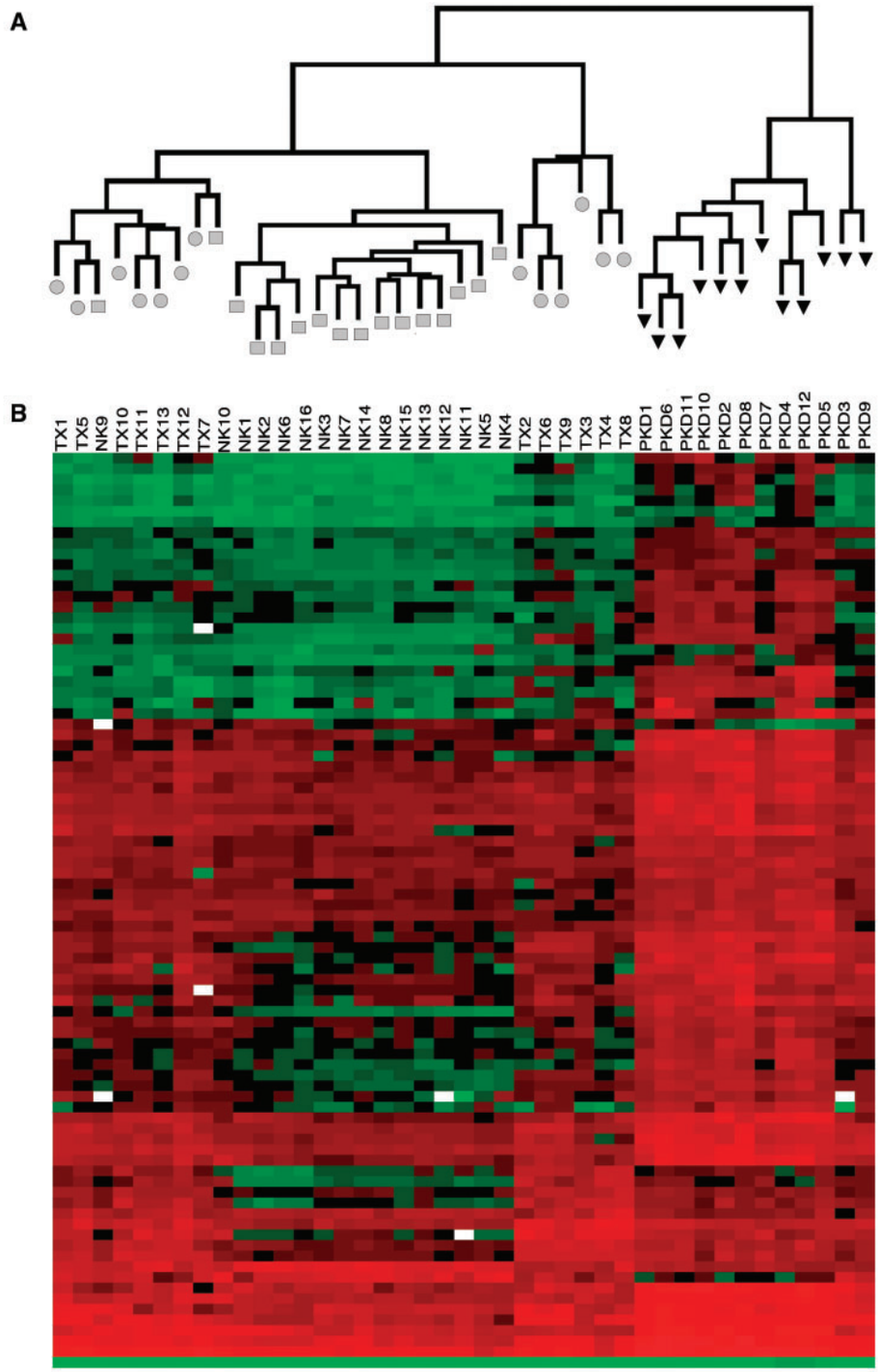

Fig. 1. Hierarchical cluster analysis of 16 normal kidneys, 13 transplant kidneys and 12 kidneys with polycystic kidney disease. Hierarchical clustering was based on genes differentiating the three tissues at a significance level of $P < 0.05$, and a more than 1.5-fold up- or down-regulation (ADPKD *vs* normal kidneys, and ADPKD *vs* chronically rejected transplant kidneys). The cluster dendrogram [Figure 1A, normal kidneys (closed circle)/ADPKD (closed triangle)/chronic allograft rejection (closed square)] and the heat map (Figure 1B, red = up-regulation/green = down-regulation) reveal that the gene expression profiles of normal, ADPKD and rejected transplant kidneys are clearly distinct.

(T×2, T×3, T×4, T×6, T×8, T×9). Thus, the dendrogram confirmed that the expression profile in end-stage ADPKD differs from normal kidneys, and is more closely related to other kidneys with ESRD.

Genes specific for polycystic kidney disease

Examining the functional categories of genes which distinguish ADPKD, we found a number of regulated genes coding for proteins involved in metabolism and homeostasis ($n=24$), signalling ($n=18$), adhesion/extracellular matrix ($n=12$), cytoskeletal proteins ($n=14$), immune response ($n=8$), transcription ($n=6$), differentiation ($n=1$) and ion transport ($n=1$). The function of three genes is currently unknown (Table 1).

Verification of differentially expressed candidate genes by RT–PCR

To confirm the differential regulation of genes found in the microarrays with a different technique, we performed semiquantitative RT–PCR on all RNA-samples of the normal and the ADPKD tissue for calponin, caldesmon, fibulin-1 and keratin 19. Although this method might underestimate the difference in gene expression, mRNA expression in cystic kidneys was clearly up- or down-regulated in ADPKD compared with normal kidneys, thus mirroring very closely the microarray data (Figures 2 and 3). GAPDH mRNA expression was used as internal control.

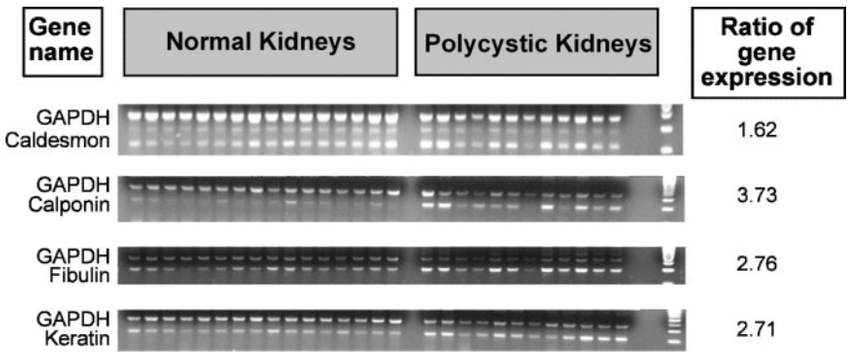

Fig. 2. Confirmation of gene expression data obtained by microarray analysis using RT–PCR. Semiquantitative RT–PCR was performed for four candidate genes. The mean of the ratios of gene expression was calculated with the Scion Image Software (Scion, Frederick, MD)

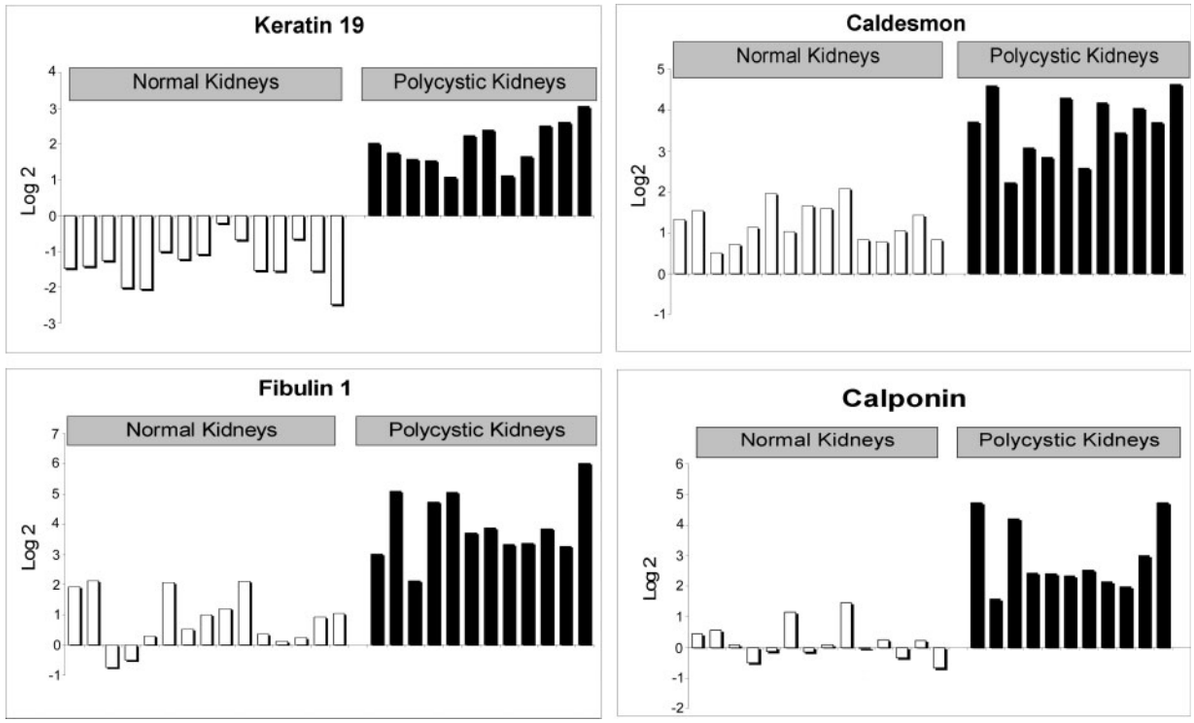

Fig. 3. According to the depiction of Figure 2, the four diagrams show the results of the microarray experiments for each of the ADPKD and normal kidney samples. Gene expression in comparison with GAPDH is given on a logarithmic scale. Microarrays and RT–PCR show comparable levels of gene regulation.

Verification of differentially expressed candidate genes by immunochemistry

To further validate the expression profiles, we performed immunohistochemistry of selected gene products. Paraformaldehyde-fixed sections of paraffin-embedded tissue of four normal kidneys and four cystic kidneys were stained for SMA, caldesmon, fibulin-1 and keratin 19. Representative results for one patient are shown in Figure 4. All four proteins were present in both cystic kidneys as well as in normal renal tissues. Keratin 19 and fibulin-1 were confined to the epithelial cells lining the cysts. In the normal kidney, both proteins were observed only in a few tubules. Consistent with its strong up-regulation on microarrays, elevated SMA and caldesmon mRNA expression was accompanied by a dramatic increase in the protein level, mainly located in the enlarged interstitium of cystic kidneys, while SMA was restricted to vascular epithelium in the normal kidney. In addition to the interstitial localization, caldesmon protein was also observed in cyst-lining epithelia in ADPKD kidneys as well as in a few discrete tubules in the normal kidney specimen.

Discussion

Although the genetic defects leading to ADPKD have been elucidated, the process that underlies progressive cyst formation and renal failure are poorly understood (see [12] for recent review). To elucidate mechanisms associated with ESRD in ADPKD, we analysed ADPKD kidneys that were removed during renal transplantation. To eliminate differential gene expression triggered by uraemia, we compared ADPKD kidneys with non-functional renal transplants. This approach eliminated genes with identical regulation in ADPKD and chronic transplant failure. Using a threshold of >1.5-fold change in gene expression at a level of $P < 0.05$, cDNA-microarray analysis

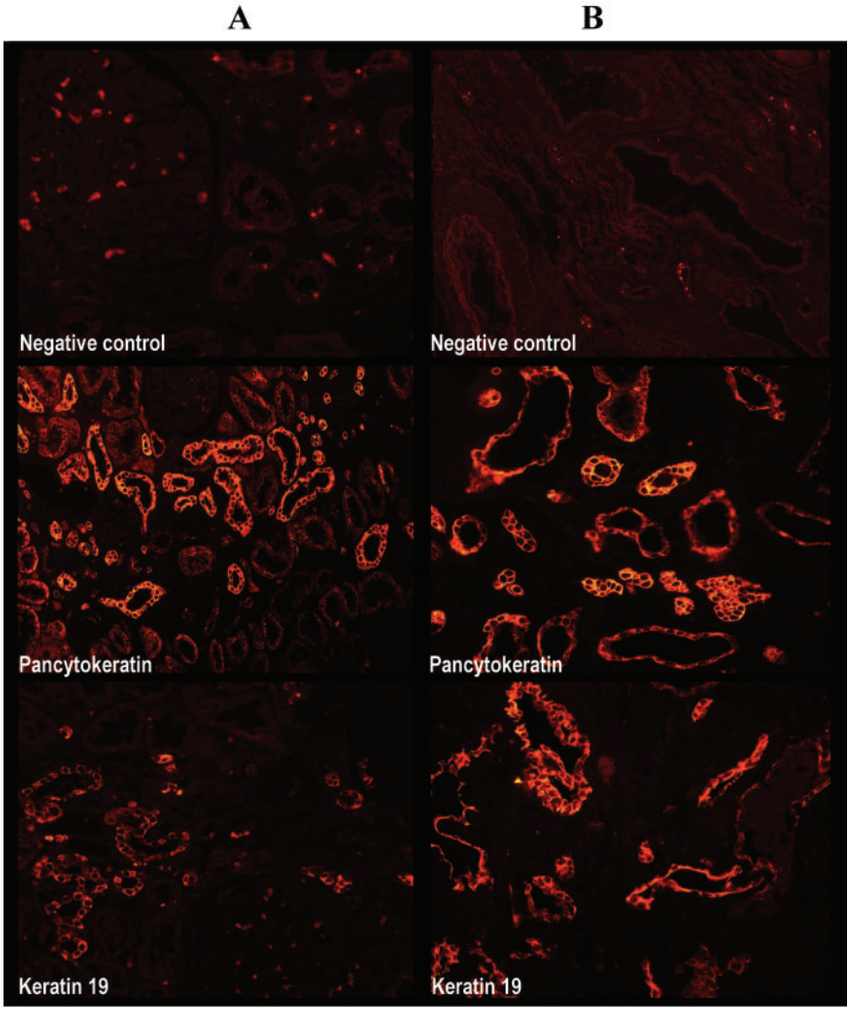

Fig. 4. Immunofluorescence of selected genes in normal and ADPKD kidneys. The staining pattern (Rhodamine Red) of representative areas in normal (**A**) and polycystic kidneys (**B**) are shown. In normal kidney tissue, fibulin-1, keratin 19 and pancytokeratin were detected only in some tubular epithelia, while these proteins were preferentially expressed in cystic epithelia of ADPKD kidneys. SMA and caldesmon were preferentially detected in the interstitium of ADPKD kidneys.

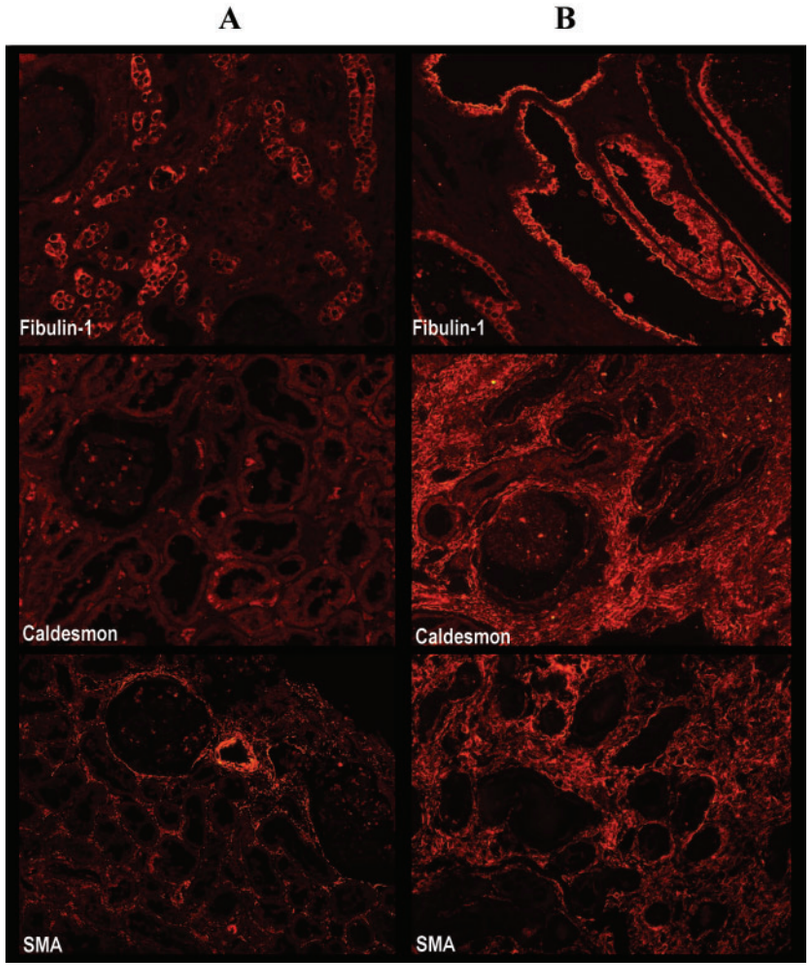

Fig. 4. Continued.

revealed significant changes for 87 ADPKD-specific genes. Although the absolute changes in expression level may not reflect their biological significance, we focused on a subset of genes with either dramatic up- or down-regulation. Cluster analysis confirmed that these genes depict a disease-specific gene expression pattern.

A recent study by Husson *et al.* [13] compared the gene expression profiles of immortalized cell lines derived from either normal or cystic kidney epithelial cells using serial analysis of gene expression (SAGE). The 205 candidate genes identified with SAGE were subsequently used for a cDNA-microarray analysis comparing ADPKD and normal kidney tissue. The results show no overlap to our data. This is not surprising, since Husson *et al.* [13] used cultured cell lines while we used tissue samples. In addition, the differences of the techniques used and the limited number of genes assessed by both methods may contribute to this discrepancy.

About 25% of the differentially regulated genes are encoded by cytoskeletal or matrix proteins as well as proteins involved in differentiation. Interestingly, a subset of genes belonged to smooth muscle-related genes suggesting that EMT contributes to the progression of renal failure in ADPKD. One EMT marker, SM22, a protein expressed at early stages of EMT, revealed a 4.33-fold increase. Using immunohistochemistry, we confirmed the RNA-based expression data at the protein level.

EMT transdifferentiation has been implicated in the process of tubulointerstitial fibrosis, and appears to represent a final common pathway of progressive kidney failure. While myofibroblasts, typically expressing SMA, are rarely found in the interstitium of normal kidneys, their number increases with disease progression, and correlates with the deterioration of renal function [14]. Growing evidence now suggests that interstitial myofibroblasts originate from tubular epithelial cells by EMT. EMT of human tubular epithelial cells can be induced by TGF-ß [15], and co-stimulation with EGF and TGF-ß induces expression of the myofibroblast-specific marker proteins, such as vimentin and FSP-1 [16]. Since cyst fluid of human ADPKD kidneys contains several growth factors, including EGF, HGF, FGF-2 and TGF-ß [17], the growth factor activities contained in cyst fluid could therefore directly trigger the EMT and the changes in gene expression reported in this study.

Caldesmon, a cytoskeleton-associated protein typically present in smooth muscle thin filaments of differentiating smooth muscle cells, was up-regulated in the interstitium and the cyst-lining epithelia of ADPKD kidneys. In IgA nephropathy, caldesmon expression correlates with advanced fibrosis [18], suggesting that up-regulation of caldesmon in ADPKD coincides with the loss of normal renal tissue.

Fibulin-1 is a calcium-binding glycoprotein, produced by mesenchymal and endothelial cells. Fibulin-1 deficiency in knock-out mice is lethal, and homozygote animals die within 24–48 h after birth, due to massive haemorrhage and endothelial dysfunction. During organogenesis, fibulin-1 is detected in mesenchymal cells involved in mesenchymal-to-epithelial transition [19]. In ADPKD kidneys, fibulin-1 was localized to cyst-lining epithelia. Since fibulin-1 interacts with the C-type lectin domains of versican and aggrican [20], fibulin-1 could directly interact with the C-type lectin present in the amino-terminal domain of polycystin-1. Thus, up-regulation of fibulin-1 could be explained by either induction of EMT, or by a missing negative regulatory feedback signal, normally triggered by an interaction between fibulin-1 and polycystin-1. A second member of the fibulin family, fibulin 4 was up-regulated in ADPKD. Fibulin-4 is found in the medial layers of large veins and arteries and in some small capillaries. Although the up-regulation of smooth muscle and cytoskeletal proteins in ADPKD kidneys likely plays no role in cyst development, the accelerated EMT in ADPKD appears to contribute to the progression of renal failure and development of ESRD in ADPKD. Growth activities contained in cyst fluid may directly contribute to EMT and the progressive renal failure of ADPKD. Thus, therapeutic strategies directed to suppress EMT may ameliorate the clinical course of polycystic kidney disease. In addition, up-regulation of other hormone and growth factor receptors such as prostaglandin E, endothelin and serotonin receptor may point to additional therapeutic targets to prevent cyst progression.

The authors wish it to be known that, in their opinion, the first two authors contributed equally to this work.

Conflict of interest statement. None declared.

References

1. Watnick T, Germino G. From cilia to cyst. *Nat Genet* 2003; 34: 355–356
2. Bycroft M, Bateman A, Clarke J *et al*. The structure of a PKD domain from polycystin-1: implications for polycystic kidney disease. *Embo J* 1999; 18: 297–305
3. Qian F, Germino FJ, Cai Y, Zhang X, Somlo S, Germino GG. PKD1 interacts with PKD2 through a probable coiled-coil domain. *Nat Genet* 1997; 16: 179–183
4. Tsiokas L, Kim E, Arnould T, Sukhatme VP, Walz G. Homo- and heterodimeric interactions between the gene products of PKD1 and PKD2. *Proc Natl Acad Sci USA* 1997; 94: 6965–6970
5. Nauli SM, Alenghat FJ, Luo Y *et al*. Polycystins 1 and 2 mediate mechanosensation in the primary cilium of kidney cells. *Nat Genet* 2003; 33: 129–137
6. Wilson PD. Polycystin: new aspects of structure, function, and regulation. *J Am Soc Nephrol* 2001; 12: 834–845
7. Woo D. Apoptosis and loss of renal tissue in polycystic kidney diseases. *New Eng J Med* 1995; 333: 18–258
8. Eisen MB, Brown PO. DNA arrays for analysis of gene expression. *Methods Enzymol* 1999; 303: 179–205
9. Boldrick JC, Alizadeh AA, Diehn M *et al*. Stereotyped and specific gene expression programs in human innate immune responses to bacteria. *Proc Natl Acad Sci USA* 2002; 99: 972–977
10. Dudoit S, Young YH, Speed T, Callow M. Statistical methods for identifying differentially expressed genes in replicated cDNA microarray experiments. *Statistica Sinica* 2002; 12: 111
11. Benjamini Y, Hochberg, Y. A practical and powerful approach to multiple testing. *J Royal Stat Soc B* 1995; 57: 289
12. Watnick T, Germino GG. Molecular basis of autosomal dominant polycystic kidney disease. *Semin Nephrol* 1999; 19: 327–343
13. Husson H, Manavalan P, Akmaev VR *et al*. New insights into ADPKD molecular pathways using combination of SAGE and microarray technologies. *Genomics* 2004; 84: 497–510
14. Alpers CE, Hudkins KL, Floege J, Johnson RJ. Human renal cortical interstitial cells with some features of smooth muscle cells participate in tubulointerstitial and crescentic glomerular injury. *J Am Soc Nephrol* 1994; 5: 201–209
15. Yang J, Liu Y. Dissection of key events in tubular epithelial to myofibroblast transition and its implications in renal interstitial fibrosis. *Am J Pathol* 2001; 159: 1465–147516
16. Strutz F, Zeisberg M, Ziyadeh FN *et al*. Role of basic fibroblast growth factor-2 in epithelial-mesenchymal transformation. *Kidney Int* 2002; 61: 1714–1728
17. Wilson PD. Aberrant epithelial cell growth in autosomal dominant polycystic kidney disease. *Am J Kidney Dis* 1991; 17: 634–637
18. Ando Y, Moriyama T, Oka K *et al*. Enhanced interstitial expression of caldesmon in IgA nephropathy and its suppression by glucocorticoid-heparin therapy. *Nephrol Dial Transplant* 1999; 14: 1408–1417
19. Zhang HY, Timpl R, Sasaki T, Chu ML, Ekblom P. Fibulin-1 and fibulin-2 expression during organogenesis in the developing mouse embryo. *Dev Dyn* 1996; 205: 348–364
20. Timpl R, Sasaki T, Kostka G, Chu ML. Fibulins: a versatile family of extracellular matrix proteins. *Nat Rev Mol Cell Biol* 2003; 4: 479–489

Received for publication: 24.10.05
Accepted in revised form: 7.2.06